Research Article **Open Access**

Piotr Napieralski and Filip Rynkiewicz

Modeling Human Pupil Dilation to Decouple the Pupillary Light Reflex

The aim of this paper is to present methods to calculate pupil size based on various parameters, such as: luminance, age, corneal flux density or monocular/binocular effect. These models allow to distinguish pupil dilation caused by the influence of light and other factors such as psychological state of participants.The developed methods were presented based on empirical data. Various researchers estimate their equations based on oculographic data obtained in the course of experiments. The presented plots are based on those equations. Different approaches can be compared to show the difference between particular models.The methods presented in this paper enable a more detailed investigation of the influence of various parameters on the pupil. It can be used to better estimate the influence of light on pupil size. The main changes occurring in pupil size, i.e. contractions and dilation, are caused by light. Other criteria such emotional arousal, cognitive processes or even memory operations can also alter the pupil, among which the decoupling of light is important. The presented approach is distinct from other similar studies because it decouples the pupillary light reflex.

DOI: DOI
Received ..; revised ..; accepted ..

Abstract:

Keywords: pupil dilatation, pupilary light reflex, eye tracking

1 Introduction

The human eye is a complex biological structure, sensitive to light and pressure. Thanks to its structure, this organ provides one of the most important senses for humans, which is vision. For million years of evolution, the mammal eye has been able to differentiate between about 10 million colors and it is possibly capable of detecting a single photon. For the purpose of this research, the anatomy of the human has been simplified (see Figure 1).

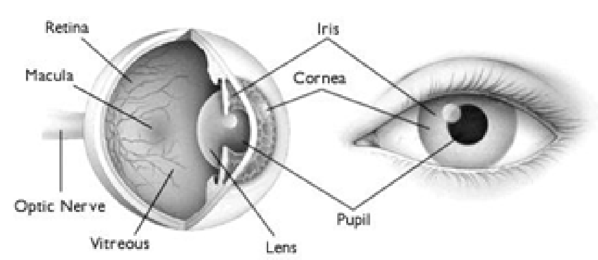

Figure: 1. Anatomy of human eye *https://goo.gl/k5qap4*

Light passes through the cornea, the pupil and the lens to finally fall on the light-sensitive cells of the retina. When the amount of light coming through the iris exceeds normal requisition, or there is shortage of light for the eye to perform normal vision, the iris sphincter muscle and iris dilator muscle react, creating what is known as the *pupillary light reflex*. The first muscle constricts the pupil when light is too bright, while the other expands it in poor light conditions. In a heightened sympathetic activity, these muscles can follow the same response pattern as in the case of various light conditions. The varying size of the pupil is a physiological response to many external factors (the pupillary response). The change in pupil size can be prompted by an involuntary reflex reaction to light (exposure to light) [1]. An increase in the size of the pupil of the eye has been found to accompany interest understood in the context of attention, and even sexual arousal [2] [3]. Other factors are memory operations [4] or a cognitive effort to distinguish between automated and controlled cognitive processing [5] [6] In normal light conditions, the pupil the pupil diameter is around 3.09mm, and 4.93mm for darkness [7]. In Figure 2, the effect of bright light and dim light is presented. As far as the latency of the light reflex, the shortest one was recorded in [8] and it was 220 ms. Some algorithms to create a virtual pupil [14] can be found in the literature, which can be used to conduct experiments without the need for human subjects.

Piotr Napieralski: Institute of Information Technology, Lodz University of Technology, e-mail: piotr.napieralski@p.lodz.pl

Filip Rynkiewicz: Institute of Information Technology, Lodz University of Technology, e-mail: 173186@edu.p.lodz.pl

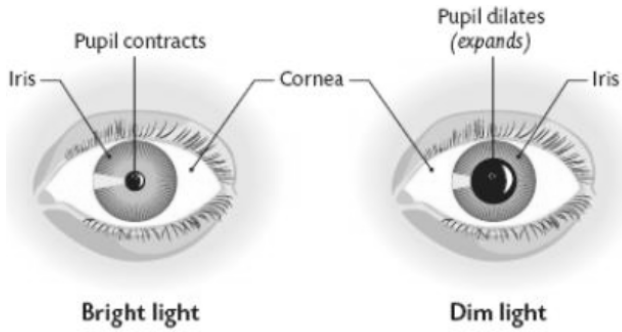

Figure: 2. Pupil dilatation based on given light [9]

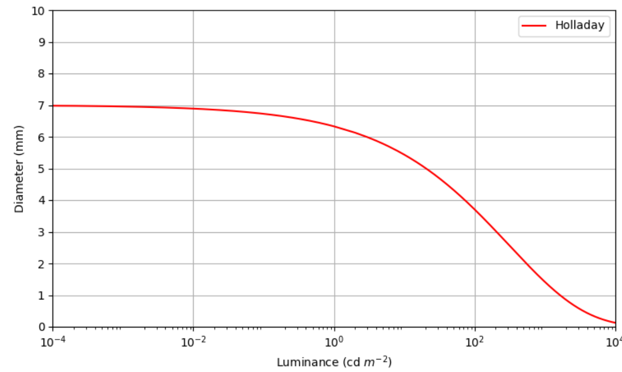

Figure: 3. Pupil size for Equation 1 of Holladay

The pupillary light reflex is modeled as a physiologically-based non-linear delay differential equation. Models of pupil changes under the influence of light may allow to separate factors related to the emotional state of the human study subject from the rate of these emotional cues. We propose to collect information about pupil dilation and then decouple the pupillary light reflex from this data. It is important to know the behavior of the eye due to changes in the light environment. Currently, studies on emotional states based on pupil size are performed in isolated laboratory environments. Accordingly, knowing and modeling pupil changes based on light conditions will allow us to isolate these changes.

2 Methods

Most models so far have been developed against the background of empirical research. Statistical models show changes in pupil size due to light reaching the eye. Based on [15], the entire equation was transformed to use **nit**(cd/m^{-2}) as the main unit of luminance. The literature describes several models built around experiments designed to measure the values of some parameters as a function of incident light intensity [10]. Calculation of pupil size based on given illumination can be performed using multiple formulas.

The first study aimed at extrapolating pupil size based on given luminance was conducted by Holladay [11]. Data was collected for 3 participants of unknown age and binocular viewing.

$$D_H(L) = 7\exp(-0.1007L^{0.4}) \tag{1}$$

$$D_C(L) = 5 - \tanh[0.61151 + 0.447\log L] \tag{2}$$

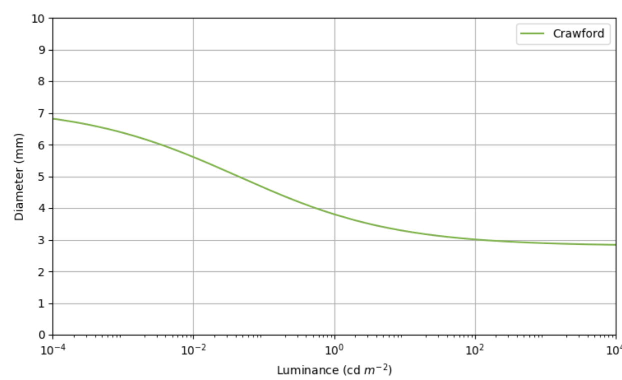

Figure: 4. Pupil size for Equation 2 of Crawford

Equation 1 plotted at Figure 3 fails for high luminance beyond $\approx 600cd/m^{-2}$ for 2mm asymptote. As in the previous study, a study by Crawford [12] also fails to reveal the age of its subjects, but their adapting field diameter is 55°. In this examination, the author took samples from 10 people. It can be observed that the asymptote of 2mm given in Holladay is not present (see Figure 4). Moon and Spencer [20], based on the equation and data approximation provided by Crawford, Blanchard [26] and Reeves [27], developed a slightly different formula, plotted in Figure 5.

$$D_{MS}(L) = 4.9 - 3\tanh[0.4\log L] \tag{3}$$

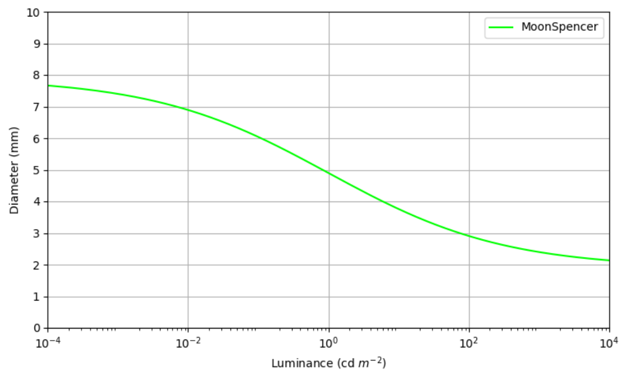

Figure: 5. Pupil size for Equation 3 of Moon and Spencer

De Groot and Gebhard [21] formulated an equation based on the averaged data from previous works, taking in consideration the number of people examined in the experiment. As can be seen in Figure 6, the asymptote of 2mm is not present in this formula either. According to the authors, it is not necessarily demanded by the data of the physiological restrictions.

$$D_{DG}(L) = 7.175 \exp[-0.00092(7.597 + \log L)^3] \qquad (4)$$

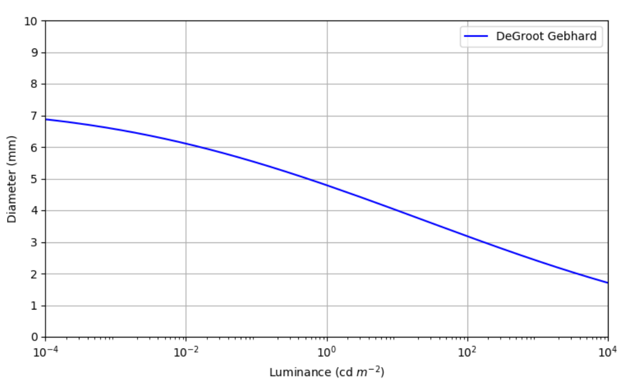

Figure: 6. Pupil size for Equation 4 of De Groot and Gebhard

Important changes in formulas were introduced by Stanley and Davies [13]. In contrast to previous works which assumed that dilatation depend only on a given luminance, they went on to conclude, based on Crawford, that the pupil diameter is directly correlated with the product of luminance L and the *adapting field size*, expressed by a in deq^2, which gives *corneal flux density*$(cdm^{-}2deq^2)$. To arrive at this formula, data was gathered from 6 volunteers whose adapting field size ranged from 0.4°to 25.4°. These two values were plotted at Figure 7 and used as thresholds for this experiment.

$$D_{SD}(L,a) = 7.75 - 5.759 \frac{(La/846)^{0.41}}{(La/846)^{0.41} + 2} \qquad (5)$$

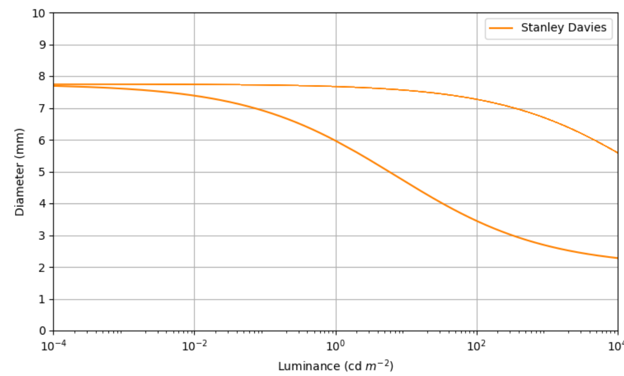

Figure: 7. Pupil size for Equation 5 of Stanley and Davies. Field diameter 0.4°(first line) and 25.4°(second line)

Barten [22] developed his own formula based on Moon and Spencer and Stanley Davies consideration of field size.

$$D_{SD}(L,a) = 5 - 3 \tanh(0.4 \log \frac{La}{40^2}) \qquad (6)$$

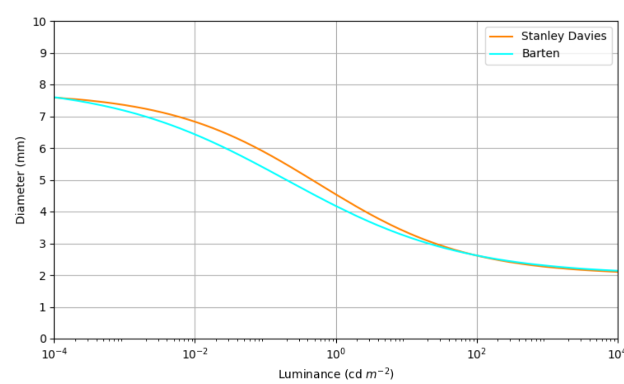

Figure: 8. Pupil size for Equation 6 Barten plotted against Stanley and Davies.

Blackie and Howland [23], based on a big project of modeling the emmetropization experiment, designed a formula expressed by:

$$D_{BH}(L) = 5.697 - 0.658 \log L - 0.07(\log L)^2 \qquad (7)$$

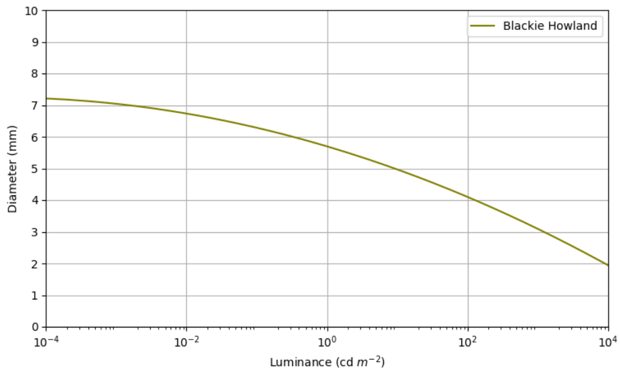

Figure: 9. Pupil size for Equation 7 Blackie and Howland.

[24] Winn carried out an experiment for 91 subjects aged from 17 to 83, including students, staff and clinical population of Aston University. Subjects maintained steady fixation at the center of an evenly illuminated circular field with a 10°diameter. Pupil diameter was measured at five luminance levels (9, 44, 220, 1100, and 4400 cdm^{-2}). The mean pupil size of 91 subjects was plotted as a function of age for five different levels of luminance. Thanks to this data, the slope and intercept were estimated. These values are given in Table 1.

Table 1. Estimated slopes and intercept for Winn etc.

cd m^{-2}	slope	intercept	r^2
9	-0.043	8.046	0.0557
44	-0.04	7.413	0.0486
220	-0.032	6.275	0.377
1100	-0.02	4.854	0.0226
4400	-0.015	4.07	0.214

Luminance was restricted to illumination in Winn et al.'s experiment. To use values from Table 1 in pupil prediction equation, the slope needs to be presented as a function of log luminance with a cubic polynomial (see Equation 8). The same pattern was followed in the case of intercept (see Equation 9).

$$
\begin{aligned}
&W_s(L) = \sum_{k=0}^{3} S_K \left(\log\left(\min\left(4400, \max\left(9, L\right)\right)\right)\right)^k \\
&s_0 = -0.24501 \\
&s_1 = -0.0368073 \\
&s_2 = 0.210892 \\
&s_3 = 0.00281557
\end{aligned}
\tag{8}
$$

$$
\begin{aligned}
&W_I(L) = \sum_{k=0}^{3} b_K \left(\log\left(\min\left(4400, \max\left(9, L\right)\right)\right)\right)^k \\
&b_0 = 6.9039 \\
&b_1 = 2.7765 \\
&b_2 = -1.909 \\
&b_3 = 0.25599
\end{aligned}
\tag{9}
$$

hen, to estimate the data of Winn et al.., both functions were combined:

$$
D_W(L, y) = W_S(L)y + W_I(L) \tag{10}
$$

where y denotes the age of a participant.

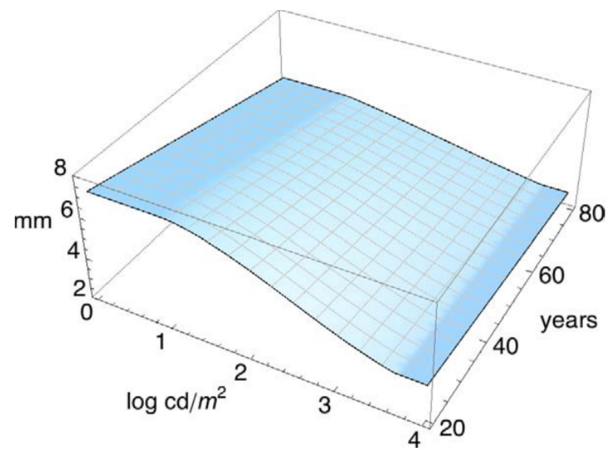

Figure: 10. Pupil size for Equation 10 off Winn.

Wattson and Yellot [15] created unified formula, which combine previously described equation and in addition giving into consideration new parameters.

Taken in account previously conducted experiments in which only dilatation of one eye was measured where the result differs from the experiments with both, given in the same adapting light (as in the Figure 11), the monocular effect was created. Based on comparison of mono and binocular data the conclusion was that the modeling of the monocular effect can be superimposed by a horizontal shift on a log axis. In which the average optimal shift of monocular data to match binocular data amounted 0.1015. With this information the factor of 0.1 can be used to shift data when in experiment only one eye is examined, and 1 when the data is collected on binocular (Equation 11)

$$
\begin{aligned}
M(1) &= 0.1 \\
M(2) &= 1
\end{aligned}
\tag{11}
$$

In addition to using the monocular effect, the *effective corneal flux density* formula was also developed, which extends the previous corneal flux density by:

$$F = LaM(e) \tag{12}$$

The result is the product of luminance, adapting area and monocular effect.

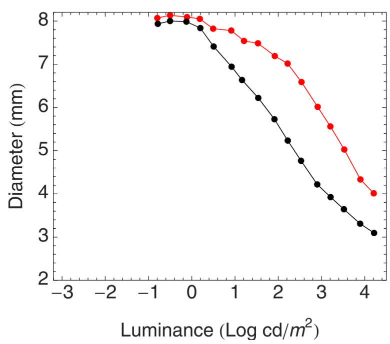

Figure: 11. Binocular and monocular data from Doesschate and Alpem [25]

In Winn et al. the age of participant was given as a crucial parameter in pupil size approximation, although data was limited to 4400 cdm^2 and the adapting field size of 10°. Assuming a linear relation between the slope function from Winn et al. and the pupil diameter calculated in Stanley Davies for the same luminance, the new general slope function could be designed.

$$S(L, a, e) = 0.02132 - 0.0095623 D_{SD}(LM(e), a) \tag{13}$$

The rate of change of the pupil diameter with age was estimated based on the function of luminance, area flux density, age, referenced age and eye function.

$$\begin{aligned} &A(L, a, y, y_0, e) = (y - y_0) S(L, a, e), \\ &20 \leq y \leq 83 \end{aligned} \tag{14}$$

Age must be in the range of that of the subjects in Winn et al. Reference age is the age of observers in the experiment. As far as reference age in the equation of Wattson Yellot, it is equal to 28.58, which is the average age of the subjects in the Stanley Davies study.

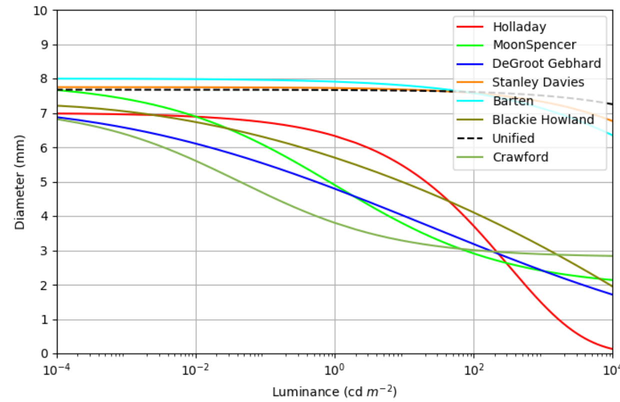

Figure: 12. Pupil size for Equation 14 of Watson and Yellot, compared to all previous models. a=10°, monocular.

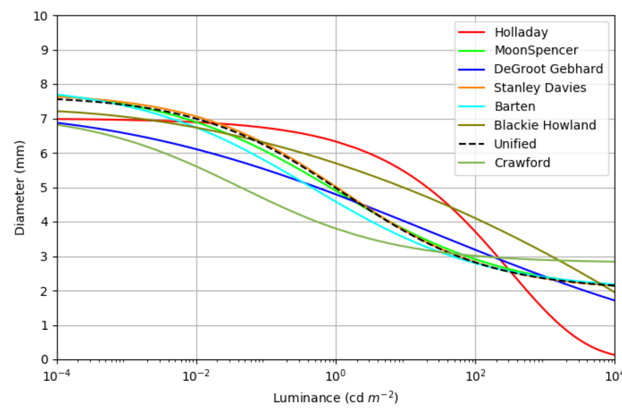

Figure: 13. Pupil size for Equation 14 of Watson and Yellot, compared to all previous models. a=60°, binocular.

Figure 12 and 13 show all the described methods and they demonstrate that these methods can differ depending on the parameters. Figure 12 presents monocular e=2 data from a small adapting area a=10. It can be seen that the Unified formula, based on Stanley and Davies, gives similar results to the Barten formula. Meanwhile In Figure 13, it can be observed that the Unified, Barten, Stanley Davies and Moon-Spencer formulas give similar results, which shows that the Watson and Yellot model can be used to predict pupil size more precisely than previous models

3 Research environment

In order to record pupil changes caused by either the internal or external factors, device called eye-tracker can be used. Main task of those devices is to track and record gaze, but in addition others vital oculography parameters can be recorded. Blink occurrence frequency, saccades detection and real time pupil size monitoring, are the most common ones. In order to record those changes multiple, either InfraRed or RGB, cameras must be used. Arrangement of those camera can be used to distinguish two main types of eye trackers.

Head-mounted eye trackers, mostly in glasses shape, have multiple cameras aimed directly onto subject eyes, and one so called global to record scene in front of the subject. The greatest advantage of these devices is their mobility, which allows subject to move freely and change locations. The biggest disadvantage is that they have lower precision and accuracy compared with stationary one, because of the subject head movement.

Second type of eye-trackers are so called remote-eye trackers. A nonintrusive peripheral device that have no contact with human body. Cameras that are placed inside this device are aimed in front of the scene, where the face of subject must be present. Those are stationary devices with no possibility to change its location, thus the test must take place in same area. The biggest advantage over wearable eye tracker is that this kind of eye tracker is nonintrusive, which is more suitable to study psychological reflexes. Thus, the device is calibrated in the way that has certain window where the eye of the subject must be visible and there are no head movement of subject the accuracy is higher in compare with wearable one.

Taking into consideration that experiment is aimed to real life scenarios like shopping, walking in the street, or event sport activity, the most important property of the device must be its mobility. Based on other researchers and solutions available in market the wearable eye tracker was chosen to this experiment. Second attribute of the device must be possibility to develop and implement new algorithms of measuring pupil changes in time. There are multiple DYI wearable eye-trackers, but they lack of precision and accuracy in comparison to solution provided in commercial solutions. Based on available devices the Tobii Pro Glasses 2, and Pupil Lab both of theme were tested in accuracy and precision. Conclusion of preliminary conducted experiment was that Tobii

Pro Glasses 2 have slightly better results than another device. Lack of possibility to extend possibilities of Tobii by adding new algorithms or another peripheral device caused that the Pupil Lab is the best choice.

This device is capable of gaze estimation with 0.6 degree of visual angle (0.08 degree precision) with a processing pipeline latency of only 0.045 seconds, blink detection, pupil size monitoring and more. The glasses-like headset eye tracker, presented at Figure 14, consist of two RGB camera with IR filter and one global directed RGB camera at the front of the user. Frontal camera is able to capture image at max resolution of 1920x1080 pixels at 30Hz with 90-degree diagonal field of view. Two IR cameras, which can operate up to 200Hz, are located at glasses frames and aimed directly to eyes of the subject. Software used in Pupil Lab uses “dark pupil” detection method thus IR cameras must be able to capture video at specific range of IR spectrum, in this device it is 860nm wavelength. Each image captured by the IR camera is analyzed by open source Pupil Lab software. Thanks to flexibility and extensibility of source code additional sensors can be added to this eye tracker. Additionally, in case of this research, to eye tracer simple luxometer was added as external sensor. The BH1603FVC Rohm analog current output ambient light sensor was used to determinate amount of light casted at pupil. It is device with compacted surface of 3.0 x 1.6 mm and spectral sensitivity close to human eye sensitivity. Sensor is capable of measuring ambient light in range of 0 - 1 000 lux on H-Gain Mode, 0 – 10 000 in M-Gain and 0 – 100 000 on L-Gain. To measure which range will be most suitable for conducted experiment the sensor was placed with 50cm range from LED lamp. This experiment gave values from 6 000 to 9 000lux , which contains in H-Gain range of sensor and in that mode sensor was calibrated. This sensor was placed near IR camera of left eye, and only this eye responses are recorder during the experiment.

(a) Pupil Lab eye tracker

(b) BH1603FVC Rohm sensor

Figure: 14. Pupil Lab eye tracker and BH1603FVC Rohm sensor. Source https://bit.ly/2TH3hby https://bit.ly/2VbrV1d

4 Conclusion

Based on the existing models, the method for measuring a light-adapted pupil diameter was implemented. We propose a solution to predict pupil size changes under visible light stimuli. The change in pupil size under the influence of light has been modeled and tested against the existing popular models. Subsequent pupillary measurements will be made with a different physiological index. We observed that the pupil diameter changes each fixation cross location in the different emotional state [16]. The magnitude of the pupil is strongly correlated with visual attention and task performance [17]. The numerical accuracy of different variants of integral image computation algorithms give the possibility of multiple evaluation of different statistical characteristics of the image [28] to extract the differences from different parameters of the pupil size. The other solution is based on artificial neural networks [18] [19] to predict the pupillary response and factor localization. We have adopted this solution due to its simplicity and generality. The results produced by our models are in agreement with observed behavior in humans and can be used in the eye-gaze tracking method in point of interest and attention estimation We believe that this work can contribute to investigations of human emotion by Human Pupil Dilation. Our results should find applicability in several areas requiring eye-tracking systems, as well as in biofeedback systems.

4.1 Application

All plots were generated in Python using the SciPy module (in particular numPy and matplotlib), which ensures the fast coding of user interface and logic of the software. In this software, the user can alter field diameter, age, mono/binocular effect and turn on/off the models to be plotted. Thanks to the built-in SciPy default Navigation-Toolbar, the user is able to create a snapshot of a plot, change its values on an axis, or manipulate the style of lines.

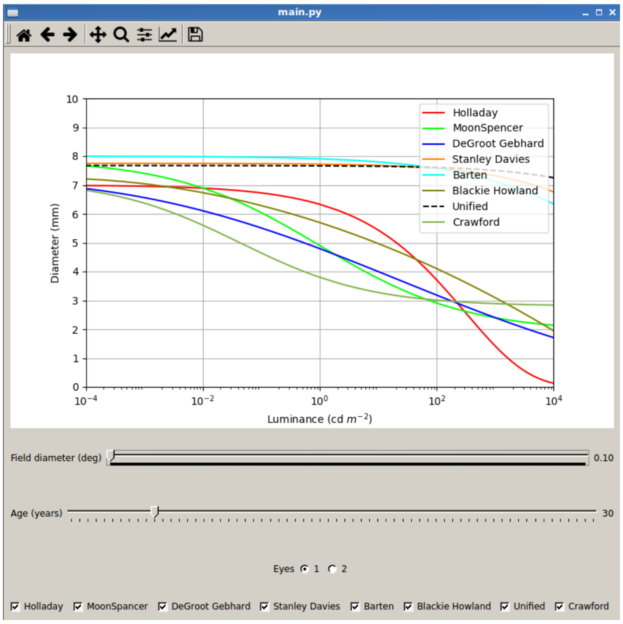

Figure: 15. Application GUI

Scripts can be found at:
https://github.com/MenosGrandes/PupilDiameter,
available freely and open-source

References

[1] Saladin K., Anatomy and physiology. New York: McGraw-Hill, 2012

[2] Hess E., and Polt J., Pupil Size as Related to Interest Value of Visual Stimuli. Science, 132(3423), pp.349-350, 1960

[3] Hammerer D., Hopkins A., Betts M., Maaß A., Dolan R. and Düzel E. Emotional arousal and recognition memory are differentially reflected in pupil diameter responses during emotional memory for negative events in younger and older adults. Neurobiology of Aging, 58, pp.129-139, 2017

[4] Bradley M., Miccoli L., Escrig M. and Lang P. The pupil as a measure of emotional arousal and autonomic activation. Psychophysiology, 45(4), pp.602-607, 2008

[5] Querino E., dos Santos L., Ginani G., Nicolau E., Miranda D., Romano-Silva M. and Malloy-Diniz L. Cognitive effort and pupil dilation in controlled and automatic processes. Translational Neuroscience, 6(1),2015

[6] Staniucha R, Wojciechowski A. Mouth features extraction for emotion classification, 2016

[7] Wyatt H. The form of the human pupil. Vision Research, 35(14), pp.2021-2036, 1995

[8] Ellis C. The pupillary light reflex in normal subjects. British Journal of Ophthalmology, 65(11), pp.754-759, 1981

[9] Walker H., Hall W. and Hurst J. (1990). Clinical methods. Boston: Butterworths.

[10] Pamplona V., Oliveira M. and Baranoski G. (2009). Photorealistic models for pupil light reflex and iridal pattern deformation. ACM Transactions on Graphics, 28(4), pp.1-12.

[11] Holladay L. The Fundamentals of Glare and Visibility. Journal of the Optical Society of America, 12(4), p.271, 1926

[12] Crawford B. The Dependence of Pupil Size upon External Light Stimulus under Static and Variable Conditions. Proceedings of the Royal Society B: Biological Sciences, 121(823), pp.376-395, 1936

[13] Stanley P. and Davies A. The effect of field of view size on steady-state pupil diameter. Ophthalmic and Physiological Optics, 15(6), pp.601-603, 1995

[14] Walraven P. The virtual pupil. Journal of Modern Optics, 56(20), pp.2251-2253, 2009

[15] Watson A. and Yellott J. A unified formula for light-adapted pupil size. Journal of Vision, 12(10), pp.12-12, 2012

[16] Raiturkar P., Kleinsmith A., Keil A., Banerjee A., and Jain E. Decoupling light reflex from pupillary dilation to measure emotional arousal in videos. SAP '16) ACM, New York, NY, USA, 89-96, 2016

[17] Ebitz R., Pearson J. and Platt M. Pupil size and social vigilance in rhesus macaques. Frontiers in Neuroscience, 8, 2014

[18] Garbaa H., Jackowska-Strumillo L., Grudzien K., Romanowski A., (2014) Neural network approach to ECT inverse problem solving for estimation of gravitational solids flow Computer Science and Information Systems (FedCSIS),

[19] Lipinski P. (2011). Watermarking software in practical applications. Bulletin of the Polish Academy of Sciences: Technical Sciences, 59(1).

[20] Moon P. and Spencer, D. (1944). The Transient Stiles-Crawford Effect. Journal of the Optical Society of America, 34(12), p.744.

[21] de Groot S. and Gebhard, J. (1952). Pupil Size as Determined by Adapting Luminance*. Journal of the Optical Society of America, 42(7), p.492.

[22] Barten P. (2000). Contrast Sensitivity of the Human Eye and Its Effects on Image Quality. Bellingham: SPIE.

[23] Blackie C. and Howland H. (1999). An extension of an accommodation and convergence model of emmetropization to include the effects of illumination intensity. Ophthalmic and Physiological Optics, 19(2), pp.112-125.

[24] Winn B., Whitaker D., Elliott D.B., and Phillips N. (1994). Factors affecting light-adapted pupil size in normal human subjects. Investigative ophthalmology & visual science, 35 3, 1132-7.

[25] Doesschate J., and Alpern M. (1967). Effect of photoexcitation of the two retinas on pupil size. Journal of Neurophysiology, 30(3), 562–576.

[26] Blanchard J. (1918). The Brightness Sensibility of the Retina. Physical Review, 11(2), pp.81-99.

[27] Reeves P. (1918). Rate of pupillary dilation and contraction. Psychological Review, 25(4), pp.330-340.

[28] Puchala D., Stokfiszewski K., Numerical Accuracy of Integral Images Computation Algorithms, IET Image Processing, vol. 12, no. 1, pp. 31-41, 2018.